1

From oil to pure water hydraulics, making cleaner and safer force feedback high payload telemanipulators

Gregory Dubus, Olivier David and Yvan Measson
CEA LIST – Interactive Robotics Unit
France

1. Introduction

One redundant characteristic of dismantling operations of nuclear facilities is the lack of exhaustive and accurate data relating to the actual state of the facilities. Most of the time the harsh working conditions (heat, dust, radiological contamination...) are rated far too severe for human workers to carry out the work. As a consequence robots are set to take over from human staff. It is necessary to use flexible, powerful and remotely-operated manipulator arms that are fitted with specially-designed processes and tools for cutting, handling and cleaning-up.

For similar reasons the maintenance of fusion reactors is another kind of application which will be carried out with help of robotic means. The International Thermonuclear Experimental Reactor (ITER) is an experimental fusion reactor based on the Russian "tokamak" concept and is the next generation of fusion machines. It will benefit of the research results on the actual existing fusion reactors to experiment long lasting pulses at high energy level. Owing to plasma interactions, some in-vessel components are expected to erode to such an extent that they will require replacement several times during the lifetime of the machine. Among these components the divertor is one of the most challenging. At the same time it has to exhaust the impurities of the plasma and to work as an actively cooled thermal shield for the lower part of the torus. But fusion reactions between deuterium and tritium isotopes produce high-energy neutron fluxes that irradiate the structure of the torus and forbid direct human access inside the reactor. As a consequence the maintenance of the in-vessel components requires the use of Remote Handling (RH) technology.

Hydraulic technology provides compact and powerful manipulators compared to electrical actuating technology. For that reason they become interesting solutions to complete maintenance and dismantling heavy duty tasks (Gravez, 2002). But decommissioning contaminated areas and operating in a fusion reactor both require a cleanliness level that oil hydraulics cannot ensure: any drop of oil inside the controlled zone must be avoided. Therefore pure water hydraulics proposes a good alternative to oil. Indeed demineralised water self evaporates in case of leakage and cannot become radioactive after radiations exposure. That's why developments are today focusing on that direction and the

development of a water hydraulic manipulator has become a key issue of both French decommissioning program and ITER maintenance program (Siuko, 2003); (Mattila, 2006).
Although basic hydraulic elements like pumps, on-off valves, filters running with pure water are already available on the market, actuators are not so many and generally limited to linear jacks. Fine control of the joint is achieved with help of servovalves. Today's off the shelf products are only adaptations from standard oil servovalves and are not specifically designed for water use. Operational experience for these products shows short lifetime expectancy and could not last a complete operating time.
Starting from the standard oil hydraulic Maestro arm, a six-degrees-of-freedom hydraulic manipulator manufactured by Cybernetix and used in decommissioning and offshore activities, CEA LIST redesigned for water applications the elbow vane actuator of the arm. Endurance tests of the Maestro vane actuator powered with demineralised water were started for identification of long term issues. Moreover, servovalves are essential components of the joint's control loop. CEA LIST evaluated the feasibility to accommodate the existing design of the Maestro oil servovalve to a prototype running with water. This prototype is a pressure-control valve. To a current input this servovalve supplies a very accurate pressure difference output instead of a flow rate in the case of flow control servovalves that are generally used in that kind of applications. The advantage is the improvement of the performances and stability of the force control loop. In addition, architecture of hydraulic manipulators with force feedback capabilities available on the market is today based on a serial arrangement of rotational joints (generally six). The replacement of one rotational degree of freedom by a linear joint, or the addition of a linear joint within the joint arrangement, could significantly improve the working range of such systems which are considered at the present time as a limiting factor for many specific RH tasks. Designing a hydraulic manipulator with a prismatic joint could therefore lead to a heavy duty multi-purpose manipulator with extended reach capabilities and alternative access to space constrained area. As a consequence, in parallel of the above-mentioned works, a new linear joint concept has been designed and proposed by CEA LIST.
This chapter first presents the complete Maestro system and then gives an overview of the development activities currently carried out to adapt its hydraulic manipulator so that it works with water instead of oil. In parts 3 and 4 both static and dynamic performances are given for the modified vane actuator and the new servovalve respectively. About the joint we also describe the results of the endurance test campaign that has been carried out. Then a design update is proposed to adapt the present design to water operating constraints with a minimum of changes. Basis of a numerical model of the servovalve is proposed in order to identify its driving parameters and validate the projected evolutions of its design. Part 5 concerns the new linear joint concept. We describe the mock-up manufactured on the proposed joint concept and the first trials with this new driving axis.

2. Overview of the Maestro system

2.1 Overall system description

The Maestro telerobotic system belongs to the class of servomanipulators, which appeared in the early 80's with the progress on computer assisted teleoperation. Compared to traditional through-the-wall workstations equipped with mechanical master-slave systems, these systems provide innovative features and improved capabilities including:

- operation from a remote control room located in an unrestricted access (cold) area
- use of different arm morphologies and technologies for the master and the slave
- work in cartesian coordinates
- compensation of the handled tools' weight
- adjustable force and speed ratios in the force feedback loop
- automatic robot modes (tool picking, return to rest position...)
- virtual mechanisms to assist operator in tricky tasks
- virtual reality to improve operator viewing
- real-time collision avoidance to protect both environment and manipulators

But if power of electric motors is enough to supply good force feedback capabilities to the operator in master arm stations, operations in the hot zone sometimes require the capability to supply high forces that standard electric motors are unable to provide in a limited space.
Starting from a hydraulic manipulator developed for offshore applications, CEA LIST developed the remote handling system Maestro (Modular Arm and Efficient System for TeleRObotics) (Dubus, 2008) for heavy duty nuclear operations (see Fig. 1).
The Maestro telerobotic system is composed of:

- a master station including:
  - a Haption Virtuose 6D master-arm
  - a master-arm controller
  - the 3D graphical supervision interface MagritteWorks, based on Solidworks
  - video display monitors
- a slave station including:
  - a 6 DOF hydraulic manipulator
  - a rad-hardened embedded slave-arm controller
  - an embedded hydraulic power pack
  - a remotely controlled PTZ video camera with tool tracking capabilities

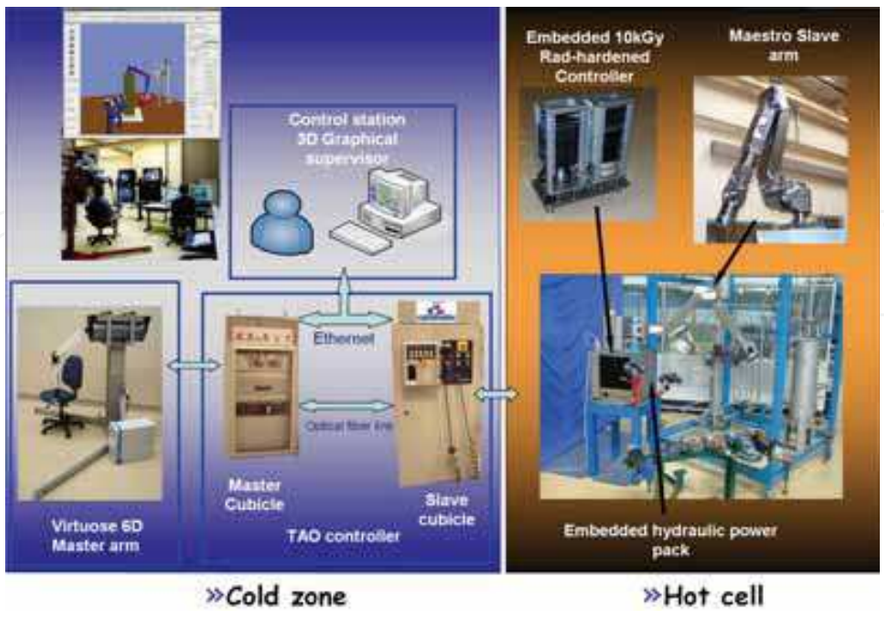

Fig. 1. Description of the Maestro system

2.2 Design of the slave manipulator

Built in titanium, the Maestro slave-arm is a 6-DOF, 2.4m-long hydraulic manipulator (see Fig. 2). Its payload capacity is up to 100 kg for 90 kg own weight. The actuator technology is based on rotary hydraulic joints. The fluid, traditionally oil, is supplied through the arm at a 210 bars pressure and a 15 L/min flow rate. The monitoring of the pressure difference between the two chambers of each joint makes it possible to drive the arm in a traditional force reflective master-slave configuration.

The system specifications were defined according to the requirements of decommissioning activities in existing nuclear facilities and maintenance scenarios of the fusion reactor ITER. Although rad-resistance of the joint itself is higher, a qualification campaign in an irradiation facility already proved resistance of the joint and its rad-hardened embedded electronic-controller to a cumulated dose of 10.65 kGy under a mean dose rate of 74 Gy/h. Special attention was paid to satisfy easy decontamination requirements, preferring smooth surfaces and avoiding any contamination traps in the design.

Qualification of the complete system for RH operations in nuclear facilities ran through a validation process including long term reliability testing. Endurance tests were carried out with different payloads during 1000 hrs. This operating time should be close to ITER needs between two shutdowns. The trajectory was defined according to position records during a representative teleoperation task including tool picking, task completion with tool, and tool removal.

Fig. 2. The Maestro manipulator

2.3 Servovalves

Servovalves are, in servo controlled hydraulic systems, the equivalent of amplifiers for electrical servomotors. Each joint is equipped with a servovalve, which controls the in and out fluid flows through the joint chambers. Servovalves generally used in that kind of robotic applications are flow control servovalves, which supply a flow rate to a current input. This category of valve is interesting in position control loops, but it needs additional sensor information when used in force control loops.

A good alternative to flow control servovalves in force control modes is the use of pressure control servovalves. In that scheme, the controlled parameter is directly linked to the force and this has a direct impact on the control loop stability. Indeed to a current input this servovalve supplies a very accurate pressure difference output instead of a flow rate in the case of flow control servovalves. From a control point of view the scheme is highly simplified as the inner loop previously needed to compute the flow according to the measured pressure is no longer needed. Therefore, improvement of force control performance (better stability and duration of the loop highly decreased) and tuning time (less parameters to adjust) is achieved.
Moreover this technical choice is also interesting from a security point of view. Indeed using these components allows removal of all pressure sensors and therefore reduces the probability of failure of the system. In the case of an electrical failure of the pressure servovalve, no pressure will be sent to the joints and the arm will fall down slowly with a minimum impact on its environment thanks to mechanical safety valves. With a flow control scheme, a pressure sensor failure would make the control system unstable, trying to compensate the ''virtual'' lack of pressure. The result would be a full speed movement of the concerned joint until the reception of an emergency signal, which could be harmful for the arm itself and its surroundings.

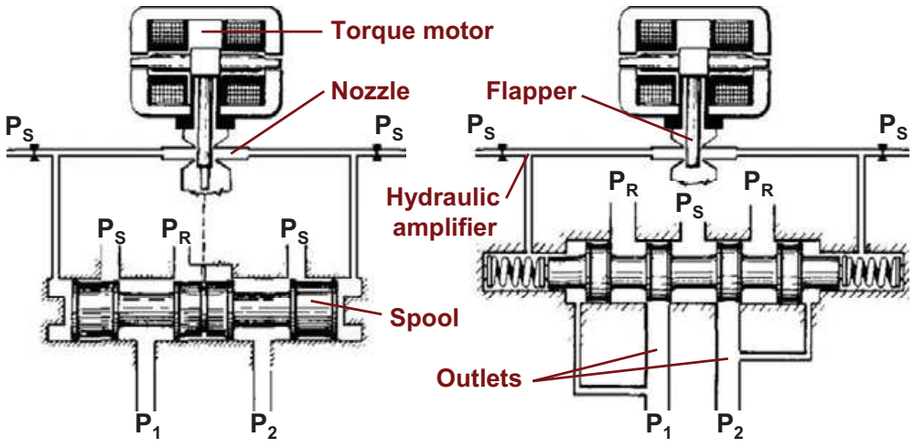

(a) (b)

Fig. 3. Principles of flow servovalves (a) and pressure servovalves (b)

The main difference between flow and pressure servovalves is the pressure feedback exerted on the spool. The two principles are shown in Fig. 3. As for a flow servovalve, the first stage of a pressure servovalve is composed of a torque motor in which the input current creates magnetic forces on both ends of the armature. The assembly {armature + flapper} rotates around a flexure tube support which moves the flapper between the two nozzles. It builds up a differential pressure proportional to the torque induced by the input current. This pressure moves the spool and opens one control port to supply pressure P_S and the other control port to return pressure P_R. The particularity of the pressure servovalve is that building-up the differential pressure (P_2-P_1) creates a feedback force on the spool, which moves backward to balance forces giving proportionality.

Prototypes of oil pressure servovalves with space and performance requirements needed by a Maestro manipulator were developed by CEA LIST. Their operating pressure was 210 bars and was obtained for a 10 mA current. The maximum linearity error was close to 10 bars and the threshold was about 3 bars, which was also the value of the hysteresis error. Their maximal flow rate (outlet to the atmosphere) was close to 11.5 L/min and the leak rate was less than 0.5 L/min. The bandwidth (167 Hz) was far beyond our requirements (20 Hz).
The integration of a complete set of pressure servovalves in the arm proved the feasibility of the concept. Achieved force control performance was better than observed with flow servovalves and it allowed a reduction of the total control loop period by a factor of two.

2.4 Force feedback

Accurate remote handling operations rely on good force feedback capabilities of the remote handling tools. Indirect vision of the operating scene introduces difficulties during maintenance tasks that can be successfully overcome with this extra sense of touch. Force feedback is provided to the operator by means of a hybrid force-position control scheme. As shown in previous works (Bidard, 2004), high quality force control can only be achieved with a good real-time compensation of all the manipulator mechanical joints imperfections, the arm inertia and the gravity (own weight, payload, tool...).

3. Redesign of the vane actuator

3.1 Specification and test rig description

The elbow joint of the Maestro manipulator is a 1300N.m. compact vane actuator with a 270° stroke, designed to withstand high radiations environment and to minimize duration of decontamination procedures.
Traditionally used with oil, the joint was analysed to adapt its design to water. Driving requirements during this adaptability study were:

- To use corrosion resistant materials
- To reduce clearances (direct impact on internal leaks due to water's low viscosity)
- To prevent contact between water and components with poor corrosion resistance
- To adapt seal materials and properties to water

The characterization of the joint was made on the test rig of Fig. 4 (Dubus, 2007).
It was composed of a Danfoss Nessie power pack, resins tanks to demineralise water directly coming from the tap, a Maestro elbow joint, a Moog flow control servovalve (type 30-417), an Arthus pancake resolver and four pressure sensors (Entran EPXT) measuring the supplied pressure, the pressure in the back-loop and the two output pressures at the outlets of the servovalve. To assess its performance different torques could be applied to the joint by means of an adjustable payload attached at its tip.
In addition, particular attention was paid to control properties and quality of the water used during the trials. Water was filtered and demineralised in a secondary circuit. The most efficient filter was a 1µm filter and conductivity was kept between 0.1µS/cm and 1µS/cm. This upper value was only obtained occasionally, when resins were saturated and needed to be replaced.

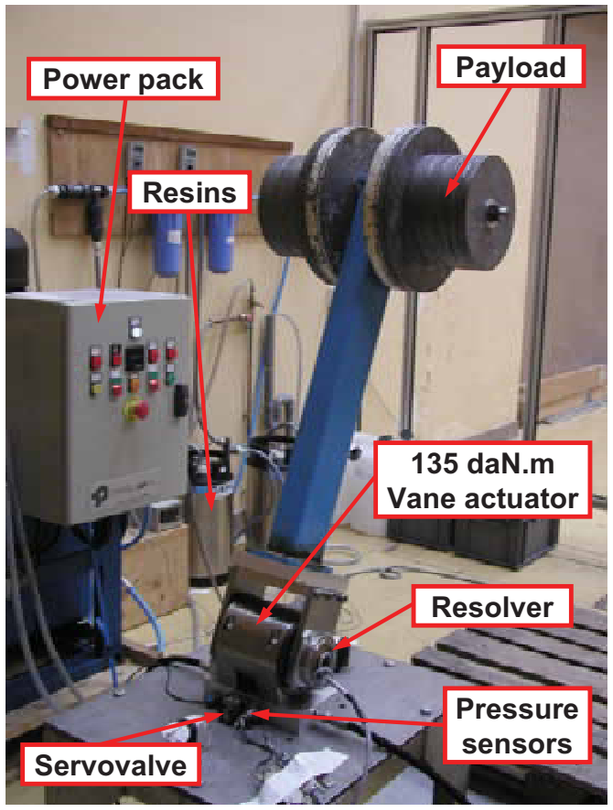

Fig. 4. Water hydraulic test bench

3.2 Characterization and performance of the hybrid force-position control

To implement a force control on the joint and assess its dynamical performance, a parametric model has been identified. As explained in paragraph 2.4, the main interest of this stage was the modelling and the identification of the friction and gravity torques, which are compensated in the force loop. A classical torque model was proposed as follows:

$$T_0 = J.\ddot{\theta} + C_v.\dot{\theta} + \text{sign}(\dot{\theta}).C_s + offset + M_x.\sin(\theta) + M_y.\cos(\theta) \quad (1)$$

In this expression J is the arm inertia, θ, $\dot{\theta}$ and $\ddot{\theta}$ are the angular position and its derivatives, C_v and C_s are respectively the viscous and dry friction coefficients, M_x and M_y represent the load among x and y axes. Being given the actuation torque, the position, the velocity and the acceleration during a position controlled sequence, the parameters were estimated thanks to a least square method. More complex models of the friction were tested, considering the joint efficiency and the effects of backdrivability as a function of the payload. But this approach had no significant impact on the identification of the main parameters. It is interesting to notice that both viscous and dry friction coefficients are 30% lower when using water instead of oil (see Table 1).

The final control scheme of the joint took into account the following compensation models: friction, gravity and rated flow (converted into torque units).

Table 2 and Table 3 present the performance for both oil and water. Obviously internal leakage is far higher in the water device. Nevertheless it seems to have a positive damping impact on the force loop dynamic performance.
Regarding the position control loop, a good tuning gives an overshoot close to 3% and the time response for a 2 rad step is close to 1 s. This value is due to the speed limitation assessed in Table 2. It corresponds to the maximum flow rate supplied by the servovalve. But compared to the 0.6 rad/s mean speed for rotary joints during standard teleoperation tasks, this performance is in agreement with the requirements.

	Oil device	Water device
Cv (N.m.s/rad)	93.0	60.1
Cs (N.m)	28.6	17.3

Table 1. Comparison between frictions of oil and water devices

	Oil device	Water device
Maximal torque (N.m)	1280	1250
Mean value of internal leak rate[a] (L/min)	0.3	1.1
Speed saturation[b] (rad/s)	2.4	2.4

[a] For the system {servovalve + joint}.
[b] Corresponds to the maximum flow rate supplied by the servovalve.

Table 2. Comparison of the static performance for oil and water hydraulic joints

	Oil device	Water device
Overshoot (%)	82	48
Time response (ms)	175	6

Table 3. Force loop performance for a 160N.m step, for oil and water hydraulic joints

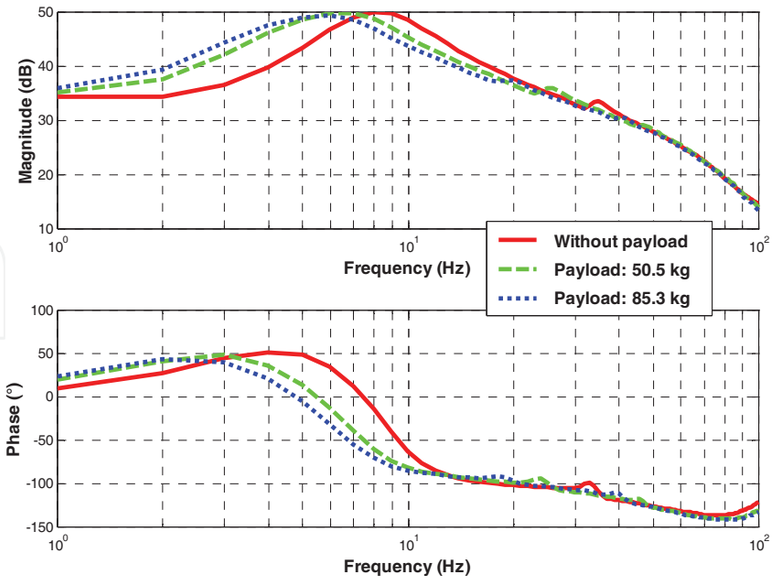

Fig. 5. Comparison of transfer functions according to payload

The torque dynamic response of the system to different payloads is given in Fig. 5. There is a reduction of the bandwidth when the payload increases, which means that it is necessary to adjust the control loop with the most critical configuration.
To evaluate the position resolution of the joint, tests were carried out at very low speed (see Fig. 6). Although the resolver resolution is very high, the position resolution of the joint is close to 0.65 mrad which is equivalent to 0.80 mm at the end-effector of the manipulator. This is due to the residual dry friction and stick slip effect that lowers the whole performance of the joint.

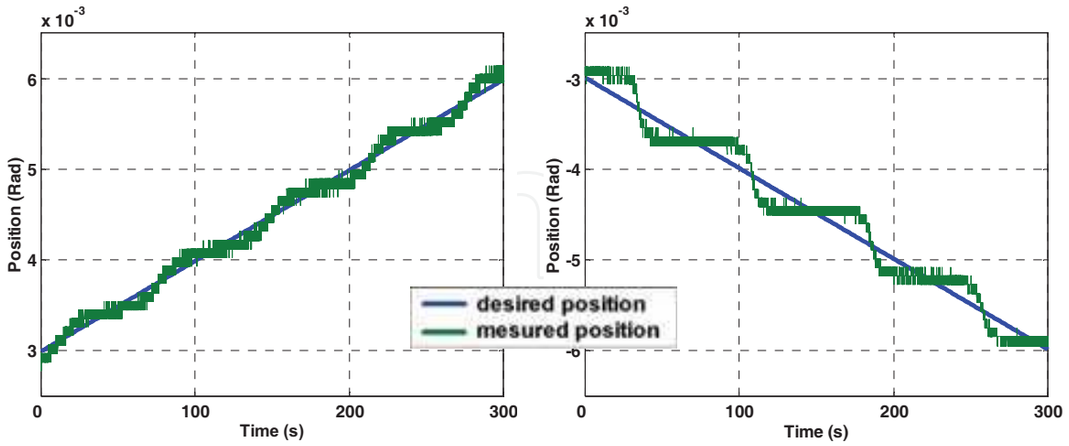

(a) (b)

Fig. 6. Very slow clockwise (a) and anticlockwise (b) movements

Reversibility tests provided a good representation of the force control loop quality when all compensation models were active (see Fig. 7). The torque peaks observed during these trials

occurred during high speed transient and they were rapidly corrected by the control scheme. Performance achieved with water was equivalent or even better than with oil.

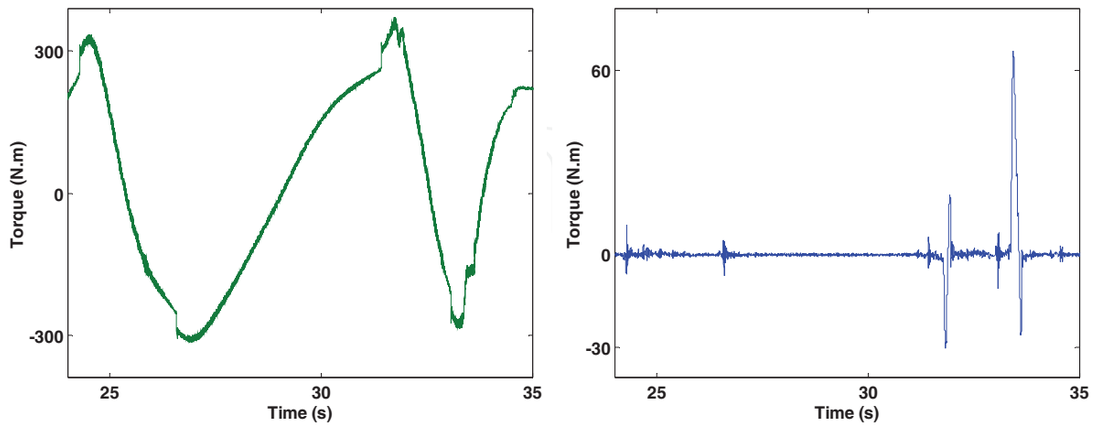

(a) (b)

Fig. 7. Reversibility test: real torque (a) and torque felt by the operator (b)

3.3 Endurance tests

As for the complete oil hydraulics arm, qualification of the joint for RH operations had to run through a validation process including long term reliability testing. 1000 hours of operation are the usual specification for the oil version of the Maestro manipulator between two stops for maintenance. This value should be close to ITER needs between two shutdowns.

The endurance tests that we performed consisted of the repetition of a single trajectory with different payload in order to simulate different manipulator configurations: with or without tool, performing a task with tool. For safety reasons, a security chain containing two limit switches and an optical watchdog were added to the test rig. Presence detection of the bar in front of the watchdog (see Fig. 8) every two minutes was necessary to avoid emergency stop.

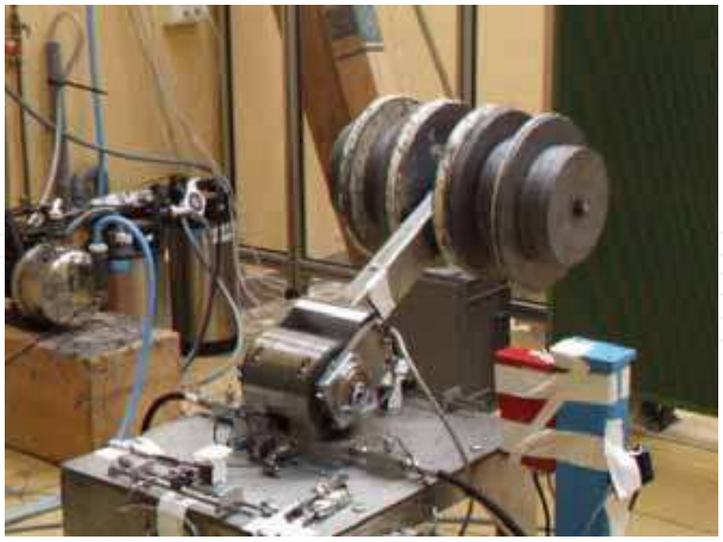

Fig. 8. Actuator in the 50daN equivalent payload configuration during endurance tests

The reference trajectory (see Fig. 9 (a)) was chosen to be representative of the movement of the Maestro elbow joint during a standard RH task such as using a shear or a circular saw. Its duration was 65 s, with mean and max speed values respectively equal to 0.21 rad/s and 0.75 rad/s. The tools' presence was simulated with adjustments of the payload. Three payloads equally distributed with time were used, each of them generating a maximal torque of 260 N.m, 545 N.m and 833 N.m respectively simulating complete manipulator configurations without tool, with a 25 kg payload, and with a 50 kg payload. Every 70 hrs the load configuration was changed.

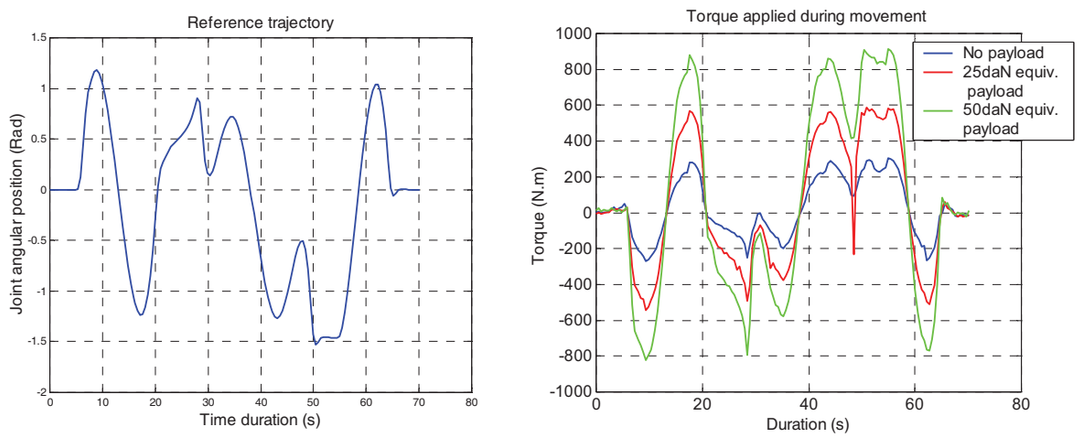

(a) (b)

Fig. 9. Reference trajectory (a) and different torque configurations (b) during endurance test

In order to detect any loss of performances, records of the current sent to the servovalves were made regularly during the trials. It was expected to detect any wear of the actuator by

an increase of this current. Indeed wear of the actuator would rapidly increase the internal leak rate, thus increasing the water flow demand to the servovalve and the current as well.

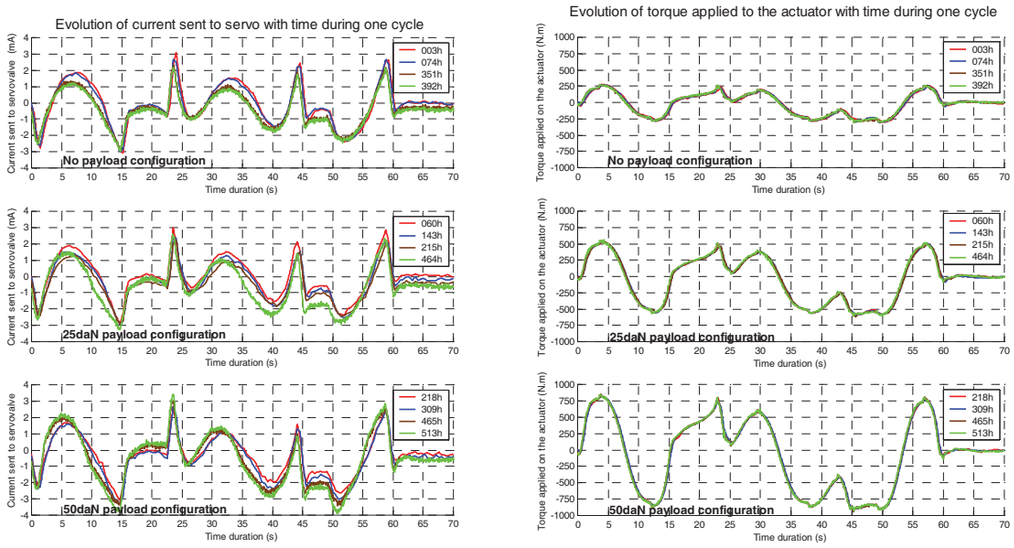

(a) (b)

Fig. 10. Current sent to servovalve (a) and measured torque (b) at different time steps

Fig. 10 presents for some cycles (random selection) the evolution of the current and the torque for all three loading configurations. Although the trajectory was always the same for the three configurations, the differences between the three configurations can be explained by the absence of inertia compensation in our control scheme.

Before every change of load a mechanical identification of the joint (dry friction, viscous friction...) was performed using the same technique as in paragraph 3.2. Variations of these mechanical parameters can usually be related to the degradation of the actuator. A modification of the viscous friction may mean an increase of the internal leakage whereas an augmentation of the dry friction may indicate a mechanical degradation of actuator.

Tests were stopped prematurely after 533h due to a consequential power pack failure. That was the second power pack failure as the distribution plate in the high pressure pump first broke around 50 hours of tests. Up to that level the MOOG servovalve was still behaving properly with no external indications of forthcoming failure.

No significant degradation of the rotary joint from both performance and mechanical points of view were noticed. Indeed the variation of both the servovalve current and the applied torque were negligible after 500 hrs. After disassembly the visual examination of the actuator didn't show any wear of the internal parts of the system. The cylinder, the vane and the flanges, which represent the main elements of the actuator, were presenting clean surfaces without corrosion spots. Seals also seemed to behave properly and were still in good physical condition. Bearings only showed that a few drops of water leaked through the drain arrangement and mixed itself with the grease but it had no consequences on the material state.

3.4 Design update

Concerning hydraulic manipulators, thorough control of the manufacturing quality and minimisation of the clearances are the main elements having an impact on the leaks. The endurance tests we performed showed that the present design of the Maestro joint was able to run at least 500 hrs without any observable degradation of its performance. To ensure the reliability of the arm up to 1000 hrs of operations, minor design updates may be considered.
New design arrangements are currently studied to minimize the impact of the change of fluid in the Maestro manipulator. These modifications have to be compatible with the existing overall design, so that the modified joint remains in a size envelope comparable to the oil version.
The main trouble that has been identified for the development of a water hydraulic arm concerns the viscosity of water. Indeed lower the viscosity, higher the potential for leaks. And external leaks would obviously result in bearing seizure. In the present Maestro design tapered roller bearings are used to withstand both the internal loads due to the fluid pressure and the external loads depending on the task in progress. These bearings are made of standard bearing steel and therefore are corrosion sensitive. Even if no corrosion has been noticed on the bearings during our tests, using such bearings without any modification of the present design could potentially affect the lifetime of the actuator.
Two technical solutions are therefore being studied to overcome this trouble:

- Integration of water compatible bearings (ceramic materials or stainless steel)
- Modification of the tightness arrangement to protect the present bearings

Results of these studies in progress should be published in future publications.

4. Development of a water hydraulic servovalve

4.1 Specification

Small size off the shelf servovalves specially developed for water hydraulic applications are unavailable on the market at the present time. The only existing products are adaptations of oil components without long term guarantee on performance and lifetime. Starting from previous results (Measson, 2003), CEA LIST launched the development of a pressure control servovalve dedicated to water hydraulic applications that fits the space constraints of a Maestro manipulator.
To meet the performance of a Maestro arm, requirements were set as follow:

- Pressure gain: 210 bars for 10 mA
- Resolution: 2 bars
- Flow rate on open ports: mini 6 L/min
- Internal leak rate: close to 1 L/min
- Bandwidth > 20 Hz

4.2 Characterization of two prototypes

As a first step, CEA LIST evaluated the feasibility to accommodate the existing design of the oil version of the servovalve to a prototype running with water. Two prototypes were manufactured. Tests were carried out on the mock-up shown in Fig. 11. This test rig was composed of a drilled block supporting the servovalve and 4 pressure sensors. Servovalve

performance is traditionally measured on closed apertures. But due to fluid compressibility, the fluid volume in both chambers acts as a spring + damper unit and affects the performance of the servovalve. That's why it was possible to connect dead volumes simulating the actuator chambers on the outlets of the servovalve.

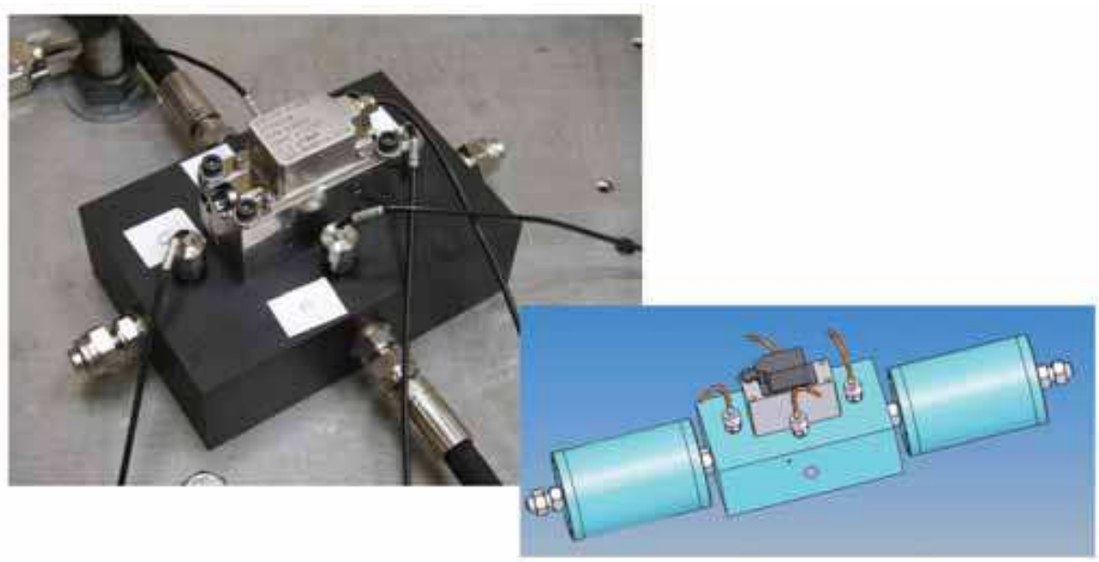

Fig. 11. Test mock-up of the water hydraulic pressure servovalve

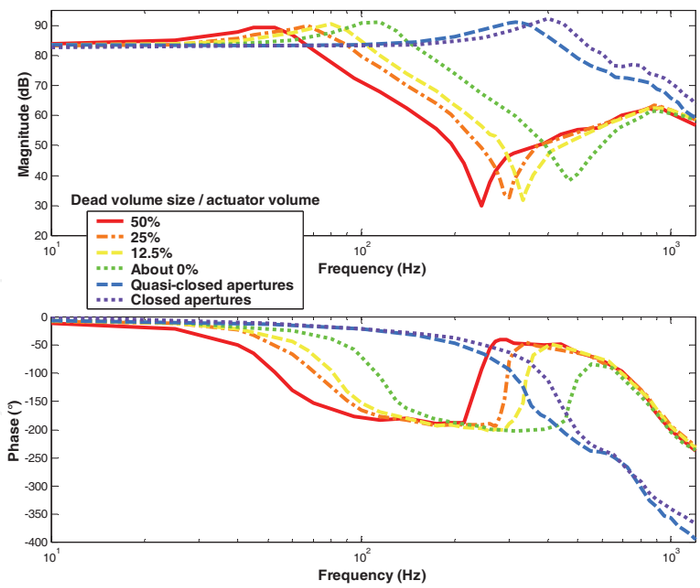

Fig. 12. Bode diagram of the servovalve for different connected volumes

The Bode diagram of the servovalve (see Fig. 12) shows a significant reduction of the valve bandwidth (ie its dynamic performance) as the dead volumes connected to the outlets of the

valve increase. But it never passes below the 20 Hz requirement. Leak rate (1.2 L/min) and flow rate (22 L/min) of the valve are close or better than the specifications but a reduction of the gain was observed. Indeed the prototype only managed to provide a 150 bars pressure difference between the 2 outlets instead of the expected 210 bars. This loss of performance was presumed to be due to an underestimated internal leakage.

4.3 Dynamic model of the pressure servovalve

To validate the above assumption, numerical models were built to identify all driving parameters of the servovalve. Starting from previous works on hydraulic systems (Merrit, 1967); (Guillon, 1992), the servovalve was divided in four subsystems. Let's establish the equations that describe the dynamic behaviour of each of these subsystems.

- Torque motor

The pilot stage consists in a torque motor and its dynamics mainly depends on the behavior of the armature-flapper assembly. The free body diagram of the armature-flapper is shown in Fig. 13 (a). We assume that the assembly moves around the pivot point *O*. The armature linear displacement is then deduced by the relation $x_f = L_n.\theta_f$. The armature-flapper is subjected to the magnetic force F_g, the pressure force at the nozzles F_n, a damping moment and a moment due to the pivot stiffness. Usually, the magnetic force F_g is found by analyzing the magnetic circuit created by the armature, the magnetic plate and the pole pieces of the torque motor. At our level, we assume that this force linearly depends on the input current and the armature displacement. At the nozzle, we can write the static pressure force as being $F_n = A_n.(P'' - P')$, where P' and P'' are the pressures that drive the spool and A_n the nozzle cross section.

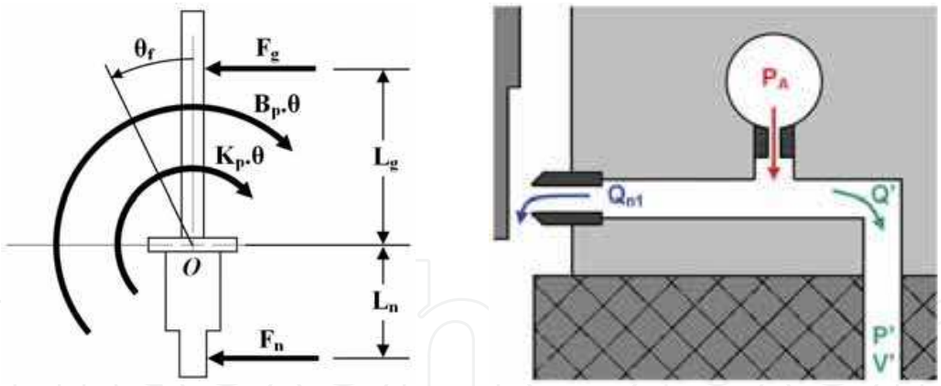

(a) (b)

Fig. 13. Free body diagram of the flapper (a) and schema of the hydraulic amplifier (b)

Summing the different moments around the pivot (Urata, 1998); (Kim, 2000), we obtain:

$$J_p\ddot{\theta}_f + B_p\dot{\theta}_f + K_p\theta_f = A_n\left(P''-P'\right)L_n + \left(K_{gf}x_f + K_{gf}i\right)L_g \tag{2}$$

According to the relation between x_f and θ, (2) gives:

$$M_f\ddot{x}_f + B_f\dot{x}_f + K_f x_f = A_n\left(P''-P'\right) + \left(K_{gf}\frac{L_g}{L_n}x_f + K_{gi}\frac{L_g}{L_n}i\right) \tag{3}$$

and leads to:

$$M_f \ddot{x}_f + B_f \dot{x}_f + K'_f x_f = A_n \left(P'' - P' \right) + K_g i \tag{4}$$

As a conclusion, for the armature-flapper assembly, we get the linear relation:

$$\ddot{x}_f = f(x_f, \dot{x}_f, P', P'', i) \tag{5}$$

- Hydraulic amplifier

Let's consider the pilot differential pressure $\Delta P_1 = P' - P''$. Pressures P' and P'' are determined by the basic hydraulic compressibility equations and the flow balance in the hydraulic amplifier (see Fig. 13 (b)). For the right part of the amplifier we get:

$$\dot{P}' = \beta \frac{Q' - \dot{V}'}{V'} \tag{6}$$

where Q' is the hydraulic flow towards the right spool chamber and V' is the volume of the chamber between the spool and the right flapper face. Its volume is therefore given by $V' = V'_0 - A_s.x_s$.

Moreover, the flow Q' into the chamber includes the flow from the supply orifice, the flow past the nozzle and the leakage past the spool. Combining the three contributions (Anderson, 2002), we get:

$$Q' = \underbrace{C_{do}\, A_o \sqrt{\frac{2}{\rho}\left(P_A - P' \right)}}_{\text{from supply orifice}} \underbrace{- C_{df}\, \pi . D_m \left(x_{fo} - x_f \right) \sqrt{\frac{2}{\rho}\left(P' - P_T \right)}}_{\text{past the nozzle}} \underbrace{- \frac{\pi . D_b\, C_r^{\,3}\, P'}{12\, \mu \left(L_{lo} - x_S \right)}}_{\text{past the spool}} \tag{7}$$

C_{do} and C_{df} are both discharge coefficient respectively for the supply orifice and the nozzle orifice. In this relation, the leakage is modeled to be a laminar flow in an annulus between an annular shaft and a concentric cylinder which initial length is L_{lo}, as it is done in (Guillon, 1992). C_r represents the radial clearance. μ is the dynamic viscosity of the fluid. In the same way, for the left part of the amplifier we get the anti-symmetric expression of Q''.

As a conclusion, for the hydraulic amplifier, we get the two nonlinear relations:

$$\dot{P}' = f(x_S, \dot{x}_S, P', x_f) \tag{8}$$

$$\dot{P}'' = f(x_S, \dot{x}_S, P'', x_f) \tag{9}$$

- Spool

The spool is subjected to the pilot differential pressure ΔP_1, a feedback force due to the load differential pressure ΔP_L, a force due to the centring springs, viscous friction and flow forces (Li, 2002). Equating these forces on the spool gives:

$$M \ddot{x}_S = \underbrace{\left(P' - P'' \right) A_1}_{\Delta P_1 \text{ force}} + \underbrace{\left(P_1 - P_2 \right) A_2}_{\Delta P_L \text{ feedback}} - \underbrace{2 K_S\, x_S}_{\substack{\text{Spring} \\ \text{feedback}}} - \underbrace{F_V}_{\substack{\text{Viscous} \\ \text{friction}}} - \underbrace{F_Q}_{\substack{\text{Flow} \\ \text{forces}}} \tag{10}$$

Assuming that the spool is perfectly centred in the bore, the viscous damping force is:

$$F_V = \mu\, A \frac{\Delta v}{\Delta y} = \mu \underbrace{\left(\pi\, d_S\, L_S \right)}_{\text{contact area}} \frac{\dot{x}_S}{C_r} \tag{11}$$

As previously, μ and C_r are respectively the dynamic viscosity of the fluid and the radial clearance. The contact area is a cylinder of diameter d_s and length L_s. The flow forces F_Q are sometimes called Bernoulli Forces and are due to the dynamics of the fluid in the spool

chambers. These forces can be split in two kinds: steady-state flow forces and transient flow forces. Steady-state flow forces are due to the angle of the average stream line when the fluid is going in or out the spool chamber. Transient flow forces are the reactive forces associated with the acceleration of the fluid in the spool chamber. According to (Merrit, 1967), these flow forces on the spool are given by:

$$F_Q = \begin{cases} \left.\begin{array}{lll} C_{dj}\, C_V\, w\left(P_A - P_1\right)\cos\alpha\, x_S & + & L_p\, C_{dj}\, w\sqrt{2\,\rho\left(P_A - P_1\right)}\,\dot{x}_S \\ + \; C_{dj}\, C_V\, w\left(P_2 - P_T\right)\cos\alpha\, x_S & - & L_p\, C_{dj}\, w\sqrt{2\,\rho\left(P_2 - P_T\right)}\,\dot{x}_S \end{array}\right\} \text{if } x_s \geq 0 \\ \left.\begin{array}{lll} C_{dj}\, C_V\, w\left(P_1 - P_T\right)\cos\alpha\, x_S & + & L_p\, C_{dj}\, w\sqrt{2\,\rho\left(P_1 - P_T\right)}\,\dot{x}_S \\ + \; C_{dj}\, C_V\, w\left(P_A - P_2\right)\cos\alpha\, x_S & - & L_p\, C_{dj}\, w\sqrt{2\,\rho\left(P_A - P_2\right)}\,\dot{x}_S \end{array}\right\} \text{if } x_s < 0 \end{cases} \tag{12}$$

In this expression the terms of the left column correspond to the steady-state forces whereas the terms of the right column are those of the transient forces. C_{dj} is the jet discharge coefficient and C_v corresponds to a velocity coefficient. Typical values for these parameters are C_{dj} = 0.61 and C_v = 2. L_p is called the damping length and represents the length of the fluid column that undergoes the acceleration. For our servo-valve, this parameter depends on the spool displacement. The angle *a*, which corresponds to the average stream line angle, is theoretically a non-linear function of x_S/C_r and varies from 21° to 69° (Merrit, 1967). A first approximation consists in fixing this parameter at its maximum value. At last, in the steady-state forces, x_S can be replaced by $\text{sign}(x_S).(x_S^2+C_r^2)^{1/2}$ in order to take into account the effect of clearance.

As a conclusion, for the spool equilibrium, we get the single nonlinear relation:

$$\ddot{x}_S = f(x_S, \dot{x}_S, P', P'', P_1, P_2) \tag{13}$$

- Controlled ports

As the spool moves in its bore, the fluid is either sucked into or out of the valve. These fluid movements have a non negligible impact on the behaviour of the servovalve. According to the flows defined in Fig. 14 (a) the flow balance in the boost stage can be written:

$$Q_1 + Q_{1F} = Q_{1S} - Q_{1R} \tag{14}$$

$$Q_2 + Q_{2F} = Q_{2R} - Q_{2F} \tag{15}$$

Q_{1F} and Q_{2F} are determined by the basic hydraulic compressibility equation:

$$Q_{1F} = \frac{dV_{1F}}{dt} + \frac{V_{1F}}{\beta}\frac{dP_1}{dt} \tag{16}$$

$$Q_{2F} = \frac{dV_{2F}}{dt} + \frac{V_{2F}}{\beta}\frac{dP_2}{dt} \tag{17}$$

To clarify the expressions of Q_{1S}, Q_{1R}, Q_{2S} and Q_{2R}, we make the choice to combine leakage and orifice flows in a single continuous relation (Eryilmaz, 2000). Therefore we get:

$$Q_{1S} = K_{1S}\sqrt{P_S - P_1}\begin{cases} (x_O + x_S) & (x_s \geq 0) \\ x_O{}^2\,(x_O - k_{1S}\,x_S)^{-1} & (x_s < 0) \end{cases} \tag{18}$$

$$Q_{1R} = K_{1R}\sqrt{P_1 - P_R}\begin{cases} x_O{}^2\,(x_O + k_{1R}\,x_S)^{-1} & (x_s \geq 0) \\ (x_O - x_S) & (x_s < 0) \end{cases} \tag{19}$$

$$Q_{2S} = K_{2S}\sqrt{P_S - P_2}\begin{cases} x_O{}^2\,(x_O + k_{2S}\,x_S)^{-1} & (x_s \geq 0) \\ (x_O - x_S) & (x_s < 0) \end{cases} \tag{20}$$

$$Q_{2R} = K_{2R}\sqrt{P_2 - P_R}\begin{cases} (x_O + x_S) & (x_s \geq 0) \\ x_O{}^2\,(x_O - k_{2R}\,x_S)^{-1} & (x_s < 0) \end{cases} \tag{21}$$

At last, theses considerations about the flow rates in the spool chambers point out an important aspect of the servovalve behaviour: the servovalve dynamics highly depends on the actuator dynamics.

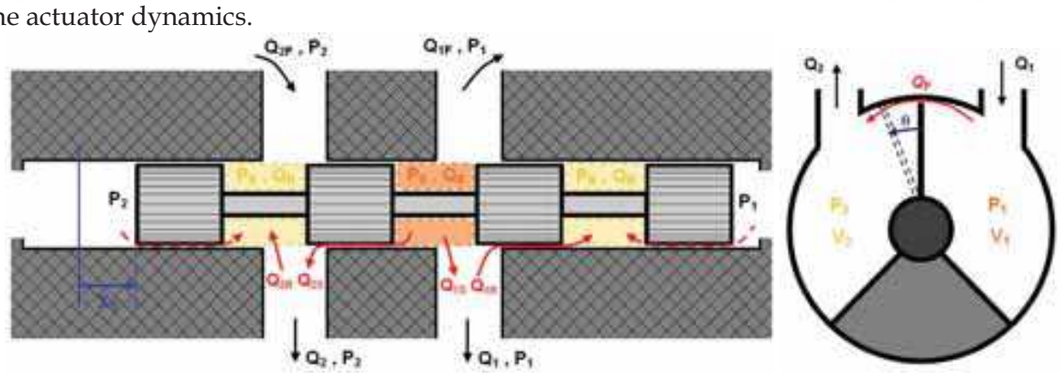

(a) (b)

Fig. 14. Free body diagrams of the spool (a) and of the rotary actuator (b)

From the hydraulic compressibility equation, we get:

$$Q_1 - Q_F = \frac{dV_1}{dt} + \frac{V_1}{\beta}\frac{dP_1}{dt} \tag{22}$$

$$-Q_2 + Q_F = \frac{dV_2}{dt} + \frac{V_2}{\beta}\frac{dP_2}{dt} \tag{23}$$

In these expressions, Q_F corresponds to the leakage from one actuator chamber to the other (see Fig. 14 (b)). Because this leakage occurs through a constant rectangular area, a simple expression for it is:

$$Q_F = C_{df}\,A_f\,sign(P_1 - P_2)\sqrt{\frac{2}{\rho}|P_1 - P_2|} \tag{24}$$

As the volumes of the two actuator chambers depend on θ the dynamics of the servovalve load differential pressure ΔP_L do as well. We can use (1) to describe the actuator dynamics.

As a conclusion, this study on the flow rates in the spool chambers leads to the eight following nonlinear relations:

$$Q_i = f(P_i, x_S, Q_{iF})_{\text{i=(1,2)}} \tag{25}$$

$$Q_{iF} = f(x_S, \dot{x}_S, P_i)_{\text{i=(1,2)}} \tag{26}$$

$$Q_i = f(\theta, \dot{\theta}, P_i, Q_F)_{\text{i=(1,2)}} \tag{27}$$

$$\ddot{\theta} = f(\theta, \dot{\theta}, P_1, P_2) \tag{28}$$

$$Q_F = f(P_1, P_2) \tag{29}$$

From the balance equations of all four subsystems, non linear systems of equations were assembled in a block diagram (see Fig. 15). Numerical solving methods were then applied to study the influence of each design parameter of the valve.

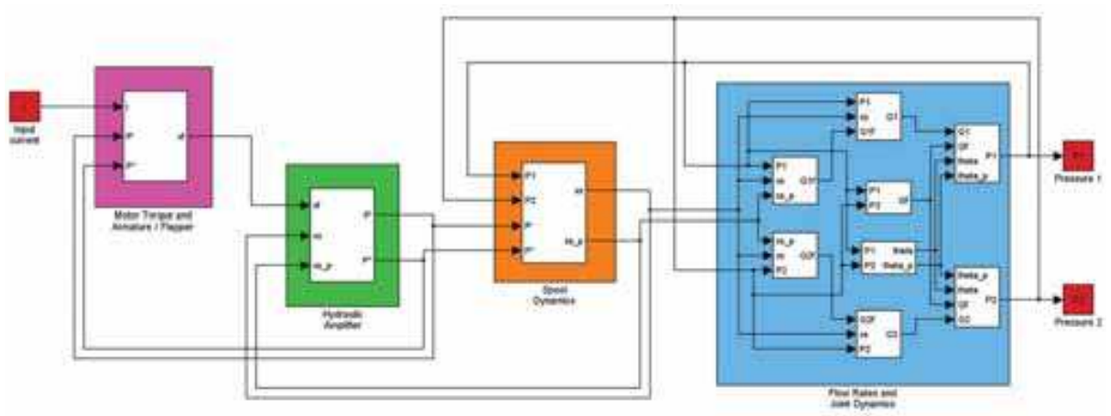

Fig. 15. Physical model block diagram of system {servovalve + joint}

This model made it possible to highlight three main dynamics corresponding to the pilot stage, the spool and the fluid compression at the outlets. We propose to express the dynamics of the entire servovalve as a simplified linear model, given by the following transfer function:

$$H(s) = \frac{K\left(\frac{s^2}{f_1^2} + 2m_1\frac{s}{f_1} + 1\right)}{\left(\frac{s^2}{f_2^2} + 2m_2\frac{s}{f_2} + 1\right)\left(\frac{s^2}{f_3^2} + 2m_3\frac{s}{f_3} + 1\right)} \tag{30}$$

To validate this model, parameters of the transfer function were evaluated thanks to the physical parameters of the block diagram system. Then the frequency response was compared with experimental results under similar conditions (see Fig. 16).

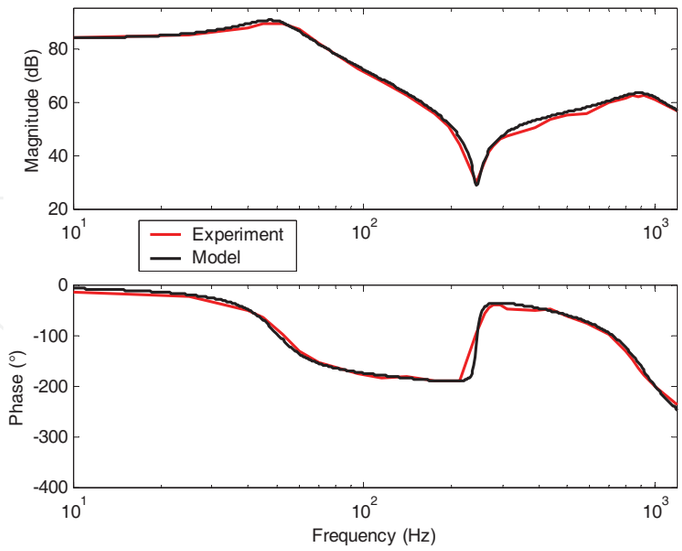

Fig. 16. Frequency response of the servovalve connected to dead volumes (75% of the volume of the actuator chamber)

This model proved that an underestimation of the leakage from the outlets toward the pilot pressure area would effectively limit the pilot forces on the spool. Solutions to reduce this effect were found but needed redesign and machining of a new prototype.

5. Development of a linear hydraulic joint

5.1 Motivation

Advanced robots architectures rely on parallel or serial arrangements of articulations. Parallel structures are used where operations require mechanics with high stiffness, transfer of high loads and high positioning accuracy. But with this kind of architecture, the workspace of the machine is limited. This is the main reason why tasks requiring high dexterity prefer serial kinematics even if wiring of the complete machine becomes a challenging task. Manipulators used for RH applications need to address a large variety of tasks and that's why dexterity is one key element for this kind of equipment.

The most common serial architecture is composed of six rotational joints in series. Orientation of all axes relatively to each other and segments' lengths are different according to the model and manufacturer. For higher dexterity the axis of three last rotations composing what is called the wrist need to be secant.

High payload Master Slave Manipulators (MSM, Fig. 17 (a)) use another alternative where the third axis is composed of a prismatic joint. The MT200 La Calhène (see Fig. 17 (b)), the CRL Model 8 or the A100 Wälischmiller are all manipulators equipped with a telescopic joint offering a 1.5 to 4m reach and a 20daN payload capacity. But limitations exist due to the cable (or metal tape) mechanisms used for both movement and force transmission. The stiffness of cables is too low to avoid extreme wrist deflection (up to 60° at full load) in some configurations during manipulation.

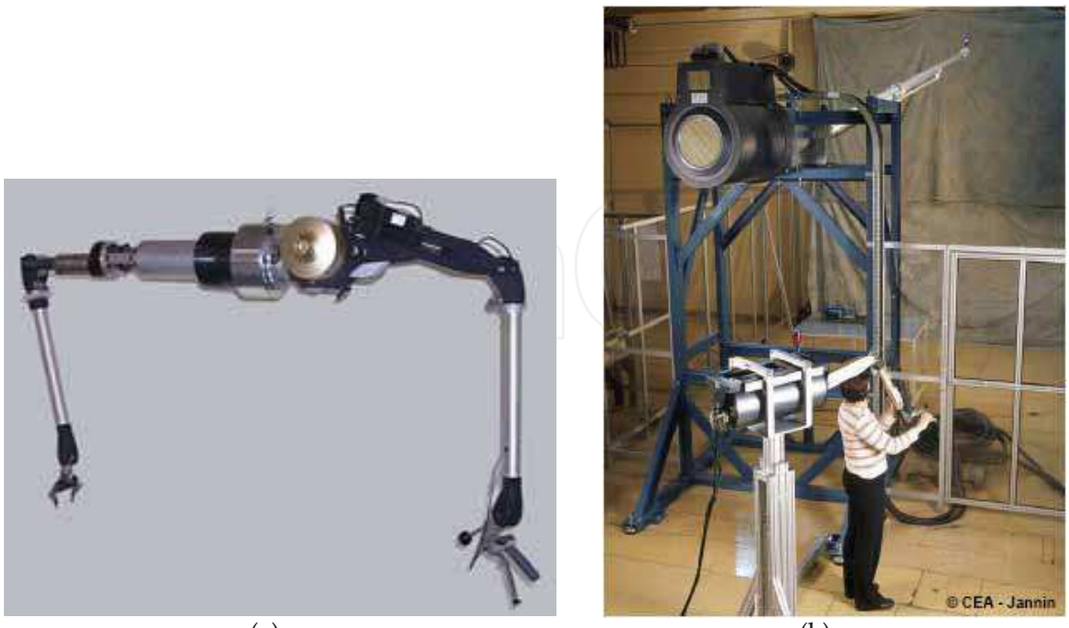

(a) (b)

Fig. 17. Examples of high payload master slave manipulator: a mechanical MSM (a) and the MT200 TAO telerobotic system (b)

The main advantage of this kinematics is to increase the workspace of the manipulator and sometimes to provide an easier access to the operating area. On the other hand, sensitivity of the force feedback is usually lower. But to keep on operating with a high dexterity level, it is commonly accepted that the position of the prismatic joint has to be upstream the three axis of the wrist.

A hydraulic manipulator having a prismatic joint has also been identified as one of the requirements for the maintenance of ITER's divertor cassettes and hot cells. To be relevant for man-in-the-loop tasks, the considered system should have the following requirements:

- Including a prismatic joint with a 1 meter stroke minimum
- High speed performance: max speed = 0.8 m/s, 0.5 m/s speed being a common value for standard displacements

Dealing with prismatic joints in the middle of a kinematics often generates a lot of difficulties for all equipment and axes that are located downstream this linear joint. Whether it is for cables (for cable powered articulations) or wires (for electric motors or measurement systems), overcoming the problem of the length adjustment is a major challenge that is not so critical for rotational joint. For hydraulic systems, the problem is the same. Supplying with fluid all downstream axes through a linear joint is far from trivial.

Two options can be followed:

- All pilot valves are located upstream the linear joint and take into account the movements of the linear joint in addition to the fluid demand of their respective axes. The control of each actuator is then linked to the control of the linear axis. Moreover the design of a proper hydraulic line for each axis is necessary. Considering that the linear joint is placed in the third position, it would mean two

pipes for each three remaining axes plus four additional pipes for the gripper and the tool changer: i.e. a total of ten pipes passing through the linear joint.
- Each pilot valve is located close to its actuator. Each actuator is independent, but a "pressure bus" with supply and return canals must run through the manipulator.

A usual solution with electric wires is to coil them in such a manner that the entire stroke of the prismatic joint is compensated by a coiling-uncoiling motion of the wire. In the same way cables in MSM systems are relying on pulley blocks arrangements for compensating the extra length adjustment during movements of the prismatic joint.
Such solutions cannot be adapted to hydraulic hoses which cannot be bent easily around small radius, especially when powered on. Moreover due to their radial flexibility it is not recommended to use hoses in the hydraulic circuit connecting the chambers of an actuator and the pre-actuator (proportional valve, servovalve). Flow and pressure variations in the chambers create second order terms in the control loop that cannot be overcome easily and decrease global stability of the system. Additionally, for safety reasons, tools designed for nuclear applications usually avoid any component such as wires or hoses outside moving bodies.
At the end of the day an efficient prismatic hydraulic joint should be such that:

- Its design avoids the use of any hydraulic hoses and must be oriented toward the use of telescopic pipes arrangement such as hydraulic jacks.
- Hydraulic circuits for supplying downstream elements should be made of two pipes providing the pressure supply at 210bars from the power pack and the return loop towards the tank.

5.2 Proposed concept

The proposed concept for the linear joint follows the principle of Fig. 18. In this arrangement the linear joint is composed of three linear jacks:

- Two passive jacks (considered as a hydraulic link between the different sections of the manipulator):
  - one jack for the hydraulic power supply
  - one jack for the return loop towards the tank
- 1 jack controlling motion and power inside the axis

The two passive jacks play the role of an extendable hydraulic circuit. They replace the rotating seal arrangement found in rotary axis. Within the joint assembly, a servovalve is connected to the pressure supply and tank return loop of the two passive jacks and controls the in and out movement of the third jack. This jack controls both force and position of the whole joint.
The main difficulty is to design a passive jack acting only as a "hydraulic link" between the two parts of the manipulator and with a minimal impact on the load supplied to the system. The difficulty is mainly due to the volume variation in each passive jack between the retracted and extended position due to the presence of the shaft on one side of the piston.
The impact of this variation for the return loop is low due to air compressibility. The air contained in the tank can adjust its volume without problem to deal with flow variations. For the high pressure fluid, the problem is more difficult during the transition from the extended configuration to the retracted configuration. During that movement a reduction of the fluid volume is necessary. Fluid can not return back within the pump of the power pack

and dealing with this extra volume requires the design of an extra system which is presented as the passive jack in the Fig. 18.

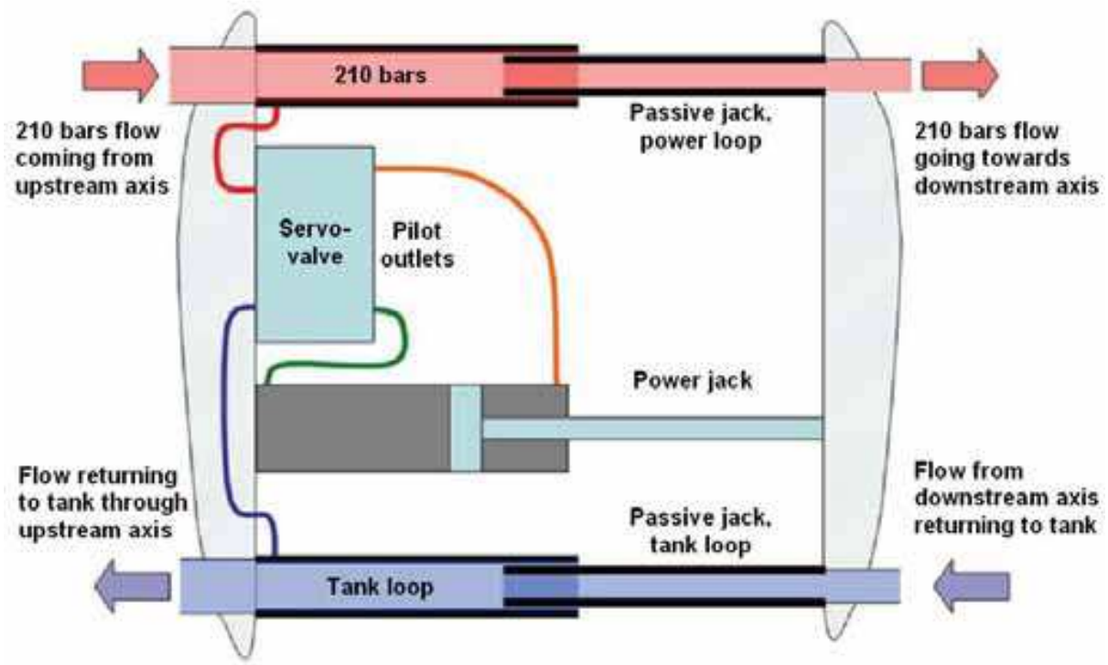

Fig. 18. Model architecture for linear joint

5.3 Preliminary tests

The test rig was designed to be modular and adaptable. The goal of these preliminary tests was to test the functions of the components and not to save space and build a fully integrated system.

Sensors and pre-actuators used for the test rig are:

- Pressures sensors : ENTRAN model EPXM-N22-350b
- Cable potentiometer: μ-epsilon WDS-1500-P60-SR-U
- Servovalve: MOOG model 4633116000

Although no force control loop has been implemented for this characterization of the joint, pressure sensors can provide information on the axial force delivered by the primary jack.

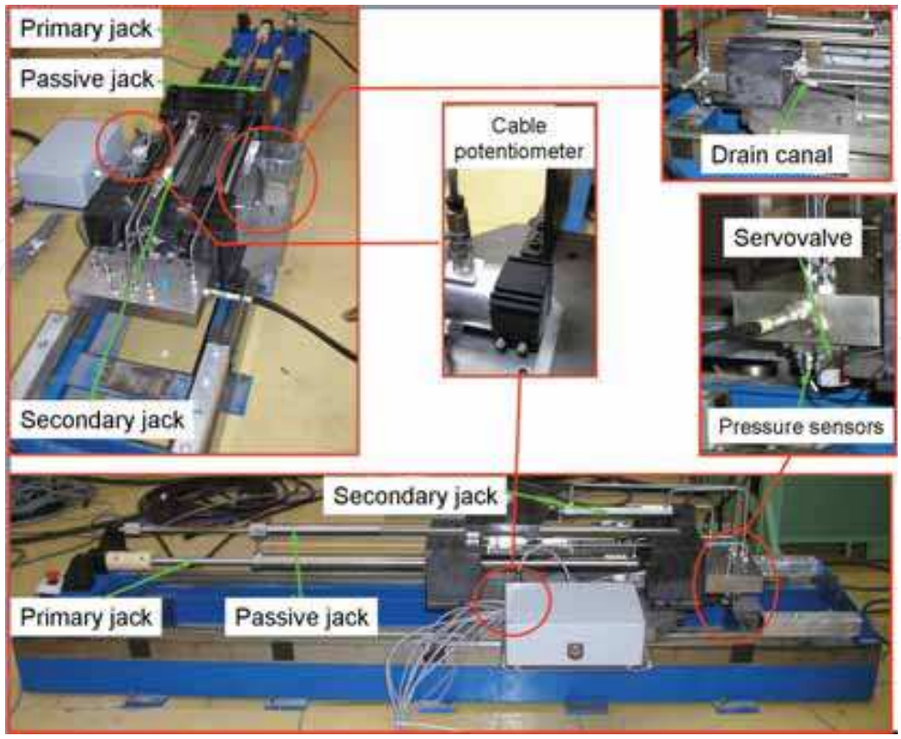

Fig. 19. Test rig

In the present design, the passive jack is one of the main components of the actuator. Due to its design and location within the system's kinematics it will act a damping system. It is therefore interesting to test the performances of the system with and without this component to characterize its influence on the whole behaviour.
Response of the actuator to a step signal is shown Fig. 20 (a). As in section 3.2 concerning the rotational link, the speed saturation is a consequence of the servovalve limited flow rate.
These results are interesting because even at the highest speed the presence of the passive jack do not seem to seriously affect the performance of the system.
Fig. 20 (b) presents the force within the primary jack when operated with and without passive jack. The reconstruction of the force was made according to the pressure values within the chambers. The results are in agreement with the expectations: both dry and viscous frictions are higher with the passive jack.

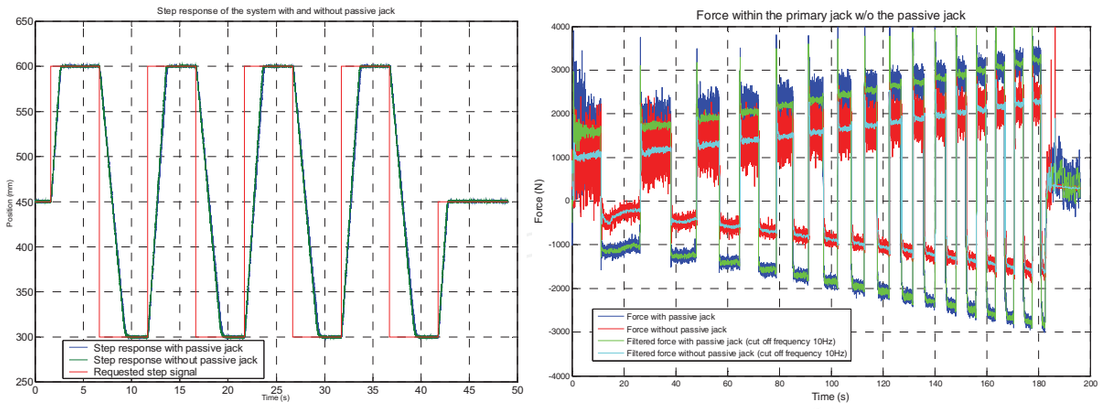

(a) (b)

Fig. 20. Position step response (a) and force measured in the primary jack (b) with and without passive jack

Asymmetry of the signal is due to the offset of the servovalve that has not been compensated yet. Moreover the oscillations noted on this force signal are due to the poor quality of the position measurement, which lead to a low quality control loop and speed oscillations. These oscillations should be reduced by a better speed measurement but creating an internal leak within the passive jack could also be another good option. Internal leaks are acting as pressure dampers and would therefore naturally filter the force within the primary jack.

As previously an identification of the system parameters has been performed to assess the force feedback capabilities of the proposed system. The test bench was configured to be used with and without the passive jack. The following table gives the values of all parameters in both configurations.

As it could be expected viscous and dry friction are higher when the passive jack is mounted on the bench. Due to its design itself (long guiding length, two concentric pipes sliding one into each other) it is not surprising to see that most of the dry friction comes from the passive jack. Viscous friction of the passive jack itself is not that high.

Parameter	Test with passive jack	Test without passive jack
Viscous friction N/(m/s)	24600	20600
Dry friction (N)	738	214
Offset (N)	305	-378

Table 4. Mechanical parameters issued from identification process

6. Conclusions

In this chapter we have tried to give the reader an overview of the studies currently carried out at CEA LIST to make hydraulic manipulators work with demineralised water instead of oil as a power fluid.

We showed that force and position performances of a Maestro elbow joint running with water are globally similar or better than the performances of the one running with oil. Minor design updates may be executed even if endurance tests proved that the joint is reliable up

to 500 hrs of operation without any observable degradation of its performance. Therefore it seems clear that the Maestro actuator becomes a very good candidate for the design of a complete water hydraulic manipulator.
Beside, pressure control water servovalve prototypes were tested with closed apertures and connected to dead volumes for qualification and characterization with water. Although most of the requirements are better or close to the expected values, the maximal pressure difference between the two ports is lower than expected. A physical model was proposed in order to identify which parameters could be responsible for this effect. Taking into account that these tests are the first ones on the first prototype generation, these results are encouraging and should foster developments in the area of water hydraulic servovalves.
At last the issue of integrating linear joint in serial architecture of hydraulic actuators has been considered. Assessment of the performances required during standard operations showed that creating a "pressure bus" within the manipulator to allow each servovalve to obtain its required fluid flow was the best answer to the problem. An innovative design was proposed. Preliminary tests on a functional mock-up have been presented and discussed.
In the next step, qualification of the water hydraulic joint equipped with a pressure servovalve instead of the flow control pre-actuator will be made. This modification would provide significant improvement of the force control loop in terms of accuracy, stability and tuning procedures. Concerning the linear actuator performance of the position measurement needs improvements to overcome limitations in the tuning of the control loop and provide a speed signal compatible with force control requirements. It is proposed to investigate the possibility to introduce data fusion procedures between two distinct sensors to reach the requested quality level.
Then the integration of all these technologies to build an extended 6DOF water hydraulic manipulator should be conceivable around 2010-2011.

7. Acknowledgements

This work, supported by the European Communities under the contract of association between EURATOM and CEA, was carried out within the framework of the European Fusion Development Agreement (EFDA). The views and opinions expressed herein do not necessary reflect those of the European Commission.

8. References

Anderson, R.T. & Perry, L.Y. (2002). Mathematical Modeling of a Two Spool Flow Control Servovalve Using a Pressure Control Pilot, *Journal of Dynamic Systems, Measurement, and Control*, Vol. 124, Issue 3, September 2002, pp. 420-427.

Bidard, C.; Libersa, C.; Arhur, D.; Measson, Y.; Friconneau, J.-P. & Palmer, J. (2004). Dynamic identification of the hydraulic MAESTRO manipulator – Relevance for monitoring, *Proceedings of SOFT23*, Venice, 2004.

Dubus, G.; David, O.; Nozais, F.; Measson, Y.; Friconneau, J.-P. & Palmer, J. (2007). Assessment of a water hydraulics joint for remote handling operations in the divertor region, *Proceedings of ISFNT8*, Heidelberg, 2007.

Dubus, G.; David, O.; Nozais, F.; Measson, Y. & Friconneau, J.-P. (2008). Development of a water hydraulics remote handling system for ITER maintenance, *Proceedings of the IARP/EURON Workshop on Robotics for Risky Interventions and Environmental Surveillance*, Benicàssim, 2008.

Eryilmaz, B. & Wilson, B.H. (2000). Combining leakage and orifice flows in a Hydraulic Servovalve Model, *ASME*, 2000.

Gravez, P.; Leroux, C.; Irving, M.; Galbiati, L.; Raneda, A.; Siuko, M.; Maisonnier, D. & Palmer, J. (2002). Model-based remote handling with the MAESTRO hydraulic manipulator, *Proceedings of SOFT22*, Helsinki, 2002.

Guillon, M. (1992). Commande et asservissement hydrauliques et électrohydrauliques, Lavoisier, Paris, 1992.

Kim, D.H. & Tsao, T.-C. (2000). A Linearized Electrohydraulic Servovalve Model for Valve Dynamics Sensitivity Analysis and Control System Design, *Journal of Dynamic Systems, Measurement, and Control*, Vol. 122, Issue 1, March 2000, pp. 179-187.

Li, P.Y. (2002). Dynamic Redesign of a Flow Control Servo-valve using a Pressure Control Pilot, *ASME Journal of Dynamic Systems, Measurement and Control*, Vol. 124, No. 3, Sept 2002.

Mattila, J.; Siuko, M.; Vilenius, M.; Muhammad, A.; Linna, O.; Sainio, A.; Mäkelä, A.; Poutanen, J. & Saarinen, H. (2006). Development of water hydraulic manipulator, *Fusion Yearbook, Association Euratom-Tekes, Annual Report 2005*, VTT Publications.

Measson, Y.; David, O.; Louveau, F. & Friconneau, J.P. (2003). Technology and control for hydraulic manipulators, *Fusion Engineering and Design*, vol.69, September 2003.

Merrit, H. E. (1967). Hydraulic Control Systems, Wiley, New York, 1967.

Siuko, M.; Pitkäaho, M.; Raneda, A.; Poutanen, J.; Tammisto, J.; Palmer, J. & Vilenius, M. (2003). Water hydraulic actuators for ITER maintenance devices, *Fusion Engineering and Design*, Vol.69, September 2003.

Urata, E. & Yamashina C. (1998). Influence of flow force on the flapper of a water hydraulic servovalve, *JSME international journal. Series B, fluids and thermal engineering*, vol. 41, no2, 1998, pp. 278-285.

IntechOpen

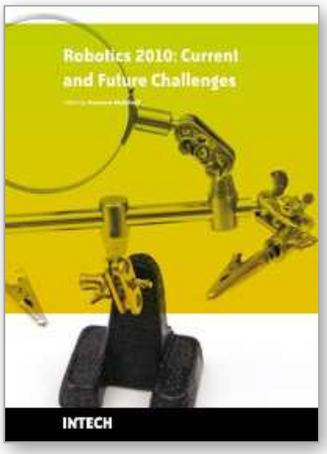

Robotics 2010 Current and Future Challenges

Edited by Houssem Abdellatif

ISBN 978-953-7619-78-7
Hard cover, 494 pages
Publisher InTech
Published online 01, February, 2010
Published in print edition February, 2010

Without a doubt, robotics has made an incredible progress over the last decades. The vision of developing, designing and creating technical systems that help humans to achieve hard and complex tasks, has intelligently led to an incredible variety of solutions. There are barely technical fields that could exhibit more interdisciplinary interconnections like robotics. This fact is generated by highly complex challenges imposed by robotic systems, especially the requirement on intelligent and autonomous operation. This book tries to give an insight into the evolutionary process that takes place in robotics. It provides articles covering a wide range of this exciting area. The progress of technical challenges and concepts may illuminate the relationship between developments that seem to be completely different at first sight. The robotics remains an exciting scientific and engineering field. The community looks optimistically ahead and also looks forward for the future challenges and new development.

InTech Europe
University Campus STeP Ri
Slavka Krautzeka 83/A
51000 Rijeka, Croatia
Phone: +385 (51) 770 447
Fax: +385 (51) 686 166
www.intechopen.com

InTech China
Unit 405, Office Block, Hotel Equatorial Shanghai
No.65, Yan An Road (West), Shanghai, 200040, China
中国上海市延安西路65号上海国际贵都大饭店办公楼405单元
Phone: +86-21-62489820
Fax: +86-21-62489821

IntechOpen